Dependence of Polyelectrolyte Apparent Persistence Lengths, Viscosity, and Diffusion on Ionic Strength and Linear Charge Density

Wayne F. Reed,*,† Snehasish Ghosh,† Ghouti Medjahdi,‡ and Jeanne François‡

Physics Department, Tulane University, New Orleans, Louisiana 70118, and Institut Charles Sadron, Strasbourg, France

Received April 18, 1991; Revised Manuscript Received July 26, 1991

ABSTRACT: Apparent electrostatic persistence lengths (i.e., those found by substituting the perturbed for the unperturbed mean-square gyration radius in the wormlike chain theory) obtained from static light scattering for variably ionized acrylamide/sodium acrylate copolymers varied approximately as the inverse square root of the ionic strength, C_s, and linearly with fractional ionization. While this does not agree directly with unperturbed persistence length theories, electrostatic excluded-volume corrections yielded better agreement with the experimental results. Intrinsic viscosity also varied as $C_s^{-0.5}$, and apparent persistence lengths extracted from those data via the Yamakawa model were in fair agreement with those from the light scattering data. In the limit of zero polymer concentration and zero scattering vector q, and equivalent hydrodynamic radius R_H was found to be independent of ionic strength, whereas the mean-square radius of gyration, $\langle S^2 \rangle$, varied strongly. This is at odds with the often-assumed linear relationship between R_H and $\langle S^2 \rangle^{1/2}$ for random coils and may imply a partial-draining condition. Finally, the "extraordinary" diffusional phase appears "removable" by filtration.

Introduction

Over the past few decades there has been a growing body of theoretical and experimental results concerning the solution properties of polyelectrolytes. The expansion of polyelectrolytes with decreasing ionic strength is a basic feature of such charged polymers. The decrease in viscosity as a function of added salt provides macroscopic verification of this. Similarly, light scattering measurements of radii of gyration and translational diffusion coefficients may be expected to reflect such changes in polyelectrolyte dimensions.

In the past, light scattering and viscosity experiments were interpreted through the Flory–Huggins theory, and the term "electrostatic excluded volume" was added to the nonelectrostatic term, the change in the local conformation being considered as a second-order effect.[1-6] Odijk[7] and, independently, Skolnick and Fixman[8] presented equivalent models for predicting the change in polyelectrolyte dimensions due to local stiffening via the dependence of the total persistence length L_T on the polymer's linear charge density and the supporting solution's ionic strength C_s. There have been several attempts to measure L_T, or at least the apparent persistence length L_T', defined in the section Estimation of Apparent Persistence Lengths. Neutron and low-angle X-ray scattering should be well-adapted for obtaining L_T directly. Unfortunately, these techniques require relatively high polymer concentration, often in the coil overlap regime and with significant addition to C_s due to the polyelectrolytes' counterions. The conclusions of such studies are sometimes contradictory. Muraga et al.,[9] for example, deduced that L_T of poly(acrylic acid) (PAA) does not depend on its degree of ionization α, while Plestil et al.[10] obtained an increase of L_T for $\alpha > 0.2$.

Light scattering[11,12] and viscosity[11,13] have been used to determine the apparent persistence lengths of several polyelectrolytes. Apparent persistence lengths have also been estimated by transient birefringence[14] measurements and studied by Monte Carlo simulations.[15,16]

Dynamic light scattering has become a standard technique for characterization of polymer dimensions. While the direct proportionality between the translational friction factor and the root-mean-square radius of gyration, $\langle S^2 \rangle^{1/2}$, predicted by the nondraining limit[17] seems fairly well-established experimentally for long, neutral polymers, recent evidence shows that this proportionality does not always hold for linear polyelectrolytes.[12,18] To confound the interpretation of dynamic light scattering data, there have also been a number of reports of an "extraordinary" diffusional phase, first for poly(L-lysine)[19] and then for other molecules such as DNA,[20,21] polystyrene sulfonate,[22] and quaternized poly(2-vinylpyridine).[23] This phase is characterized by a long scattered intensity autocorrelation relaxation time component at no added salt and low added salt, which becomes shorter as salt is added and finally gives way to the much quicker autocorrelation decay time characteristic of the "ordinary" phase at higher ionic strengths. In some studies both phases could be measured simultaneously at low ionic strength.[21,23,24]

The acrylamide/sodium acrylate copolymers are good candidates for illustrating these problems. Their charge parameter ξ can be almost continuously varied from zero to unity, and the monomer distribution is well-known.[25] They constitute a model of weakly charged polyelectrolytes with a polar, nonionic part. There are many experimental works dealing with the conformational and thermodynamic properties of the uncharged polyacrylamide.[26-29] It has been shown that polyacrylamide in water behaves as a nonpolar polymer in organic solvent. Its Θ point in water is −8 °C, and at room temperature there is a crossover between Gaussian and excluded-volume statistics. The dependence of the radius of gyration and intrinsic viscosity on the molecular weight, ξ, and salt concentration C_s has often been interpreted only in terms of excluded-volume theory.[30-32]

This work reports results on light scattering and viscometry experiments on variably ionized polyacrylamide which yield (1) apparent persistence lengths and second

† Tulane University.
‡ Institut Charles Sadron.

0024-9297/91/2224-6189$02.50/0 © 1991 American Chemical Society

virial coefficients as a function of C_s and ξ, (2) diffusion coefficients as a function of C_s and polymer concentration C_p, and (3) intrinsic viscosity as a function of C_s and ξ. Measurements and observations concerning the so-called extraordinary phase are also presented.

Summary of Salient Notions. The wormlike chain model[33] expresses the unperturbed mean-square radius of gyration $\langle S^2\rangle_0$ of a polymer in terms of total persistence length L_T and its contour length L ($L = Mb/m$, where M and m are the polymer and monomer mass, respectively, and b is the monomer–monomer countour bond length).

$$\langle S^2\rangle_0 = LL_T/3 - L_T^2 + 2L_T^3/L - 2(L_T^4/L^2)(1 - e^{-L/L_T}) \quad (1)$$

Odijk[7] and Skolnick and Fixman[8] broke the polymer's total persistence length into an intrinsic portion L_0 (due to the natural rigidity of the molecule from rotameric, steric, and possible secondary structure features) and the electrostatic portion L_e

$$L_T = L_0 + L_e \quad (2)$$

Their electrostatic persistence length is given by

$$L_e = (1/12)(q^2/d_\epsilon k_B T)N^2(3y^{-2} - 8y^{-3} + e^{-y}(y^{-1} + 5y^{-2} + 8y^{-3})) \quad (3)$$

where k_B is Boltzmann's constant, N is the number of charges on the polyelectrolyte chain, q is the magnitude of the individual charges, d_ϵ is the medium's dielectric constant, and $y = L\kappa$. κ is the Debye–Hückel screening parameter and is proportional to the square root of the ionic strength C_s. In the limit $L \gg L_T$, L_e can be expressed as a function of κ and ξ, the Manning charge parameter[34] ($\xi = q^2/d_\epsilon b' k_B T$, where b' is the intercharge spacing).

$$L_e = \xi^2/(4\kappa^2 d_B) \quad (4)$$

d_B is the Bjerrum length ($=q^2/d_\epsilon k_B T$) and is equal to about 7.18 Å at 25 °C. The relationship between the perturbed mean-square radius of gyration, $\langle S^2\rangle$, and the unperturbed mean-square radius of gyration, $\langle S^2\rangle_0$, is often expressed in terms of the static expansion factor α_s

$$\langle S^2\rangle = \alpha_s^2\langle S^2\rangle_0 \quad (5)$$

In excluded-volume theories for neutral polymers, α_s depends on hard-core steric repulsions and other short-range interactions. At low ionic strength, α_s in the polyelectrolyte case, however, may be expected to be dominated by the long-range screened Coulomb potential and is thus qualitatively different from the neutral case.

An ad hoc treatment for electrostatic excluded-volume effects obtained by combining theories of Odijk,[7] Odijk and Houwaart,[35] Fixman and Skolnick,[36] and Gupta and Forsman[37] was presented in an earlier work.[15] Since the polyelectrolytes studied here have large A_2 values even at very high C_s, we extend that treatment here by including the hard-core excluded volume in the analysis.

Odijk and Houwaart[35] proposed that the electrostatically charged wormlike chain can be approximated by a random coil having $N_k = L/2L_T$ segments, a segment length of $L_k = 2L_T$, and an electrostatic excluded-volume parameter z_{el}. With that specification the total excluded-volume parameter z is given by

$$z = (3/2\pi L_k^2)^{3/2}\beta N_k^{1/2} \quad (6)$$

where $\beta = \beta_{el} + \beta_0 + \beta_a$ and represents the excluded volume between segments, given by the sum of the electrostatic contribution β_{el}, the hard-core intersegment repulsion β_0, and any attractive interaction β_a. While β_0 should increase with decreasing C_s, β_{el} is found experimentally to become quickly much larger than β_0 with decreasing C_s, so that, for simplicity in the current work, β_0 will be approximated by its high ionic strength value under all conditions.

Odijk and Houwaart suggested computing β_{el} as the electrostatic excluded volume between two rods of length $2L_T$. Fixman and Skolnick[36] found

$$\beta_{el} = 8L_T^2\kappa^{-1}\int_0^{\pi/2}\sin^2\theta\int_0^{w/\sin\theta}x^{-1}(1 - e^{-x})\,dx\,d\theta \quad (7)$$

where $w = 2\pi(N/L)^2 d_B\kappa^{-1}e^{-\kappa d}$, d being the rod diameter. While several forms for computing α_s exist, recent Monte Carlo results[15] show the Gupta and Forsman form[37] generally works well for $N_k \geq 2$.

$$\alpha_s^5 - \alpha_s^3 \cong \frac{134}{105}(1 - 0.885N_k^{-0.462})z \quad (8)$$

The electrostatic excluded-volume effect should also appear in the behavior of A_2 vs C_s. Here the calculation can be made using Yamakawa's[17] eq 21.5

$$A_2 = (N_A N_k^2\beta/2M^2)h_0(\tilde{z}) \quad (9)$$

where

$$h_0(\tilde{z}) = [1 - (1 + 3.903\tilde{z})^{-0.4683}]/1.828\tilde{z} \quad (10)$$

and eq 21.16 in ref 17 defines $\tilde{z}$ as

$$\tilde{z} = z/\alpha_s^3 \quad (11)$$

which serves an an approximation for the effect of intramolecular excluded volume on A_2.

Experimentally determining A_2 vs C_s allows extrapolation to the high salt limit of A_2, denoted as $A_{2,hs}$. With $A_{2,hs}$ on the left side of eq 9 and the value of the apparent intrinsic persistence length L_0', obtained by extrapolation of L_T' to infinite high ionic strength, β_0 and the high salt value of α_s, denoted $\alpha_{s,hs}$, can be found numerically using eqs 6, 8, and 9–11. With $\alpha_{s,hs}$ the true intrinsic persistence length L_0 can be found, so that β_0 and β_{el} can be taken simultaneously into account in calculating theoretical values of L_T' and A_2 vs C_s. This procedure is described in more detail in the Results and Discussion. Since A_2 is large and positive, the attractive contributions to β embodied in β_a are ignored.

The effect of polymer dimensions on the translational friction factor f has been extensively investigated via the Kirkwood–Riseman[38] and Rouse–Zimm[39] models and renormalization group theory.[40] f can be found by

$$f = k_B T/D_0 \quad (12)$$

where D_0 is the value of the translational diffusion coefficient at zero polymer concentration.

For unperturbed polymers there is a fair consensus on the forms of f in the so-called "free-draining" and "non-draining" limits.[17] In the former case it is expected that $f \propto M$, while in the latter $f \propto M^{0.5}$ (in the coil limit) and also $f \propto \langle S^2\rangle^{1/2}$. Various theories exist for taking excluded volume and partial draining into account in calculating f or α_H, the hydrodynamic expansion factor.[41] α_H gives the relation between f in good solvent conditions and f_0 in the unperturbed state

$$f = \alpha_H f_0 \quad (13)$$

It has become clear that α_s/α_H is not universal.[17,41]

Yamakawa and Fujii[42] derived approximate semiempirical expressions for the intrinsic viscosity of stiff chains without excluded volume $[\eta]_0$ by applying the Oseen–Bur-

gers[43,44] procedure to wormlike cylinders

$$[\eta]_0 = \frac{\phi_0 M^{0.5}}{(M_L/2L_T)^{3/2}}\left[1 - \sum C_i\left(\frac{L}{2L_T}\right)^{-i/2}\right]^{-1} \quad (14)$$

where ϕ_0 is the theoretical Flory constant (for infinitely large molecular weight, $\phi_0 = 2.87 \times 10^{23}$ if $[\eta]_0$ is expressed in $cm^3\ g^{-1}$), and M_L is the mass per unit length ($=m/b$). The C_i's are dependent on $d/2L_T$ and can be calculated from expressions given by Yamakawa and Fujii[42] for different d/L ranges. In the free-draining limit $[\eta]_0$ is directly proportional to the molecular weight. In the nondraining limit

$$[\eta]_0 = 6^{3/2}\phi_0\langle S^2\rangle_0^{3/2}/M \quad (15)$$

In this case $[\eta]_0$ scales as $M^{0.5}$. Exponents higher than 0.5 are interpreted as arising from excluded-volume effects, as the draining effect is assumed to be negligibly small for ordinary flexible chains. Flory and Fox[45] proposed replacing $\langle S^2\rangle_0$ by $\langle S^2\rangle$ and ϕ_0 by ϕ in eq 15 (which assumes that ϕ is independent of excluded volume). With these substitutions the viscosity expansion factor, α_η^3, is then defined as

$$[\eta] = [\eta]_0\alpha_\eta^3 \quad (16)$$

Kurata and Yamakawa[46,47] developed the variation of ϕ with z in the nondraining limit:

$$\phi = \phi_0 - 0.46\phi_0 z \quad (17)$$

From this analysis it turns out that α_η^3 must be smaller than α_s^3 for positive z according to the following semiempirical expression:

$$\alpha_\eta^3 = \alpha_s^{2.43} \quad (18)$$

Weill and des Cloizeaux,[48] starting from the Kirkwood theory, have demonstrated that the intrinsic viscosity may be expressed as

$$[\eta] \propto \langle S^2\rangle R_H \quad (19)$$

and have rewritten eq 18 in the form

$$\alpha_\eta^3 = \alpha_s^2\alpha_H \quad (20)$$

This last expression seems to be in better agreement with experiments on uncharged polymers than other theories. It must be pointed out that these relations between viscosimetric, static, and dynamic expansions are strictly applicable to expanded coils and perhaps are not adaptable to the wormlike chain case. However, there have been several attempts to calculate $[\eta]$ of DNA on this basis: for instance, Odijk[49] has derived $[\eta]$ by combining the Weill–des Cloizeaux theory[48] with the excluded-volume model of the worklike chain[35] and obtained good agreement with the experimental data. Sharp and Bloomfield[50] used the Flory theory to treat the same problem, also with reasonable agreement.

Materials and Methods

Materials. The polyelectrolytes were copolymers of acrylamide and sodium acrylate, produced by photoinitiated free-radical polymerization.[51] Degrees of ionization were determined by potentiometric titration, elemental analysis, and ^{13}C NMR.[24] Table I gives a summary of the different degrees of ionization and the corresponding charge parameter ξ (determined simply as $\xi = \tau d_B/2.56$ where τ is the molar fraction of acrylate units, and 2.56 Å represents the monomer contour length). The weight-average molecular weight for all of the substances was found by static light scattering to be around 5×10^6.

Table I
Designations for the Variably Ionized Polyacrylamide/Polyacrylate Polymers with Their Fractional Ionization, τ, and Corresponding Manning Charge Parameter, ξ

polymer	fraction ionization	Manning charge param	polymer	fraction ionization	Manning charge param
AD10	0.015	0.043	AD27	0.17	0.48
AD17	0.07	0.20	AD37	0.27	0.77

The polymers were dissolved in pure water (conductivity less than 1 μS) at their own pH at 10^{-4} g/L and left to hydrate at room temperature for at least 48 h with very slow, gentle stirring. The viscosity of the salt-free solutions was so large that it was excessively difficult to filter the solutions through even 0.45-μm filters. Even after 8 h of centrifugation at 10 000g the solutions were still found to be filled with "dust" and aggregates that severely distorted the data. This problem was solved by placing the solutions in centrifuge tubes in a water bath at 90 °C for around 20 min and then immediately centrifuging them at 10 000g for 2 h. After the centrifugation had stopped the samples were still warm and could be optionally filtered through 0.22-μm membranes. Such samples were very clean and contained virtually no residual dust or aggregates. Losses in concentration due to filtering such samples were followed by measuring the change in absorbance at λ = 210 nm on the shoulder of the (incomplete) UV peak and were typically on the order of 5–20%.

Measurements of the scattered intensity $I(q)$ were made for a given polymer concentration to which were added small quantities of NaCl stock solutions. In reference to the total univalent electrolyte concentration, C_s (in mM) will be used hereafter

$$C_s = [\text{NaCl (mM)}] + [\text{AD (mg/mL)}]\tau/0.002m \quad (21)$$

where m = 71 is taken as the weight per charge group for AD and τ is the fractional ionization.

Apparatus. Static and dynamic light scattering experiments were performed on a home-built apparatus in New Orleans which has been previously described.[52] A vertically polarized argon ion laser operating at 488 nm was used. The data collection algorithm for the static scattering was modified so that at each angle a selectable number of scattered intensity readings (typically 100) were made, from which only the lowest reading was accepted as the true scattering intensity at that angle. This minimized the effect of any residual dust and aggregates, especially at low angles. Since the scattering volume contained many coherence areas and the sampling time was several tenths of seconds per point, the minima obtained by this method were not spuriously lowered by correlated interference effects at the phototube surface. Likewise, the number of photon detection events producing the detector current was high enough so that the Poisson width of the distribution of readings was negligibly narrow (less than 1% of the average count as verified from counting of filtered toluene at similar intensity levels) compared to the fluctuations resulting from random dust and aggregates wandering in and out of the scattering volume (variations up to several hundred percent of the minimum count).

Estimation of Apparent Persistence Lengths. A simple method for estimating apparent persistence lengths L_T' from the angular intensity of light scattered by solutions successively titrated with salt was used. The term "apparent" is used because no account is taken of excluded volume. Operationally, L_T' is the value of L_T found from eq 1 for a given contour length when $\langle S^2\rangle_0$ is replaced by the measured, perturbed $\langle S^2\rangle$. The method has been previously described[12] and is summarized here.

Figure 1 shows an example of the resulting curves of Kc/I vs $\sin^2(\theta/2)$ at different C_s for such a series of experiments on 0.22-μm-filtered AD17. K is given by

$$K = 4\pi^2 n^2 (dn/dc)^2/N_A\lambda^4 \quad (22)$$

where N_A is Avogadro's number, n the index of refraction of the solvent, λ the laser vacuum wavelength (488 nm), and dn/dc the differential index of refraction. This latter quantity was measured to be 0.168 and showed no measurable variation within error bars from 0 to 1 M C_s for the different ADs.[53]

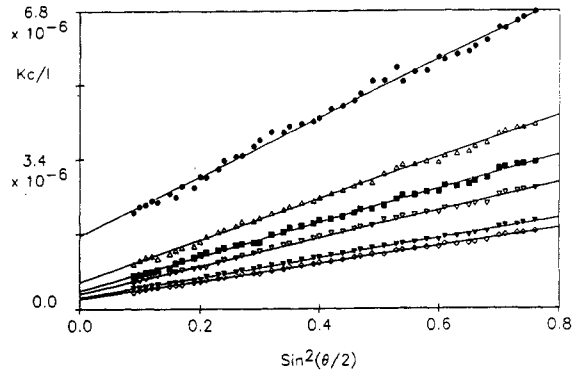

Figure 1. Kc/I for different C_s for 0.1 mg/mL of AD17: (●) 1 mM; (▲) 3.5 mM; (■) 7 mM; (▽) 15 mM; (▼) 75 mM; (◇) 500 mM.

The assumptions made in estimating the apparent persistence lengths are the following:

(1) The polymers scatter like ideal Gaussian chains

$$P(u) = \frac{2}{u^2}(e^{-u} + u - 1) \tag{23}$$

where $q = (4\pi n/\lambda) \sin(\theta/2)$ and $u = q^2\langle S^2\rangle$. Excluded-volume effects are considered in the Results and Discussion.

(2) We use for the light scattering by a polydisperse population

$$Kc/I(q) = \frac{\int mN(m)\,dm}{\int m^2N(m)\,P(q,m)\,dm} + 2A_2Q(q)\,c \tag{24}$$

where $N(m)$ is the number distribution of the molecules, and $Q(q)$ is a complicated function of intermolecular interactions.

(3) The slope of Kc/I vs q^2 in isoionic dilution is independent of c for $c < c^*$ (c^* is the overlap concentration); that is, $Q(q)$ = constant. We take $Q(q) = 1$.

(4) The radius of gyration in the absence of excluded-volume effects is related to the apparent persistence length of the polymer through the wormlike chain model by eq 1, and since experimental evidence indicates that, for this high molecular weight AD, $L_T/L \ll 1$ under all conditions studied, the molecules are assumed to be near the coil limit and

$$\langle S^2\rangle_0 \cong LL_T/3 \tag{25}$$

However, since light scattering measures $\langle S^2\rangle$, the apparent persistence length L_T' is computed when $\langle S\rangle^2$ is substituted $\langle S^2\rangle_0$ in eq 26.

$$\langle S^2\rangle = LL_T'/3 = \alpha_s^2LL_T/3 \tag{26}$$

Since $\alpha_s^2 \geq 1$, L_T' is an upper limit on the true persistence length L_T.

(5) If u is large enough that $e^{-u} \ll 1$ for the whole population (in practice u should be larger than about 3), then to second order in u^{-1}

$$Kc/I(q) \cong 1/2M_n + \gamma q^2/2 + 2A_2c \tag{27}$$

where the relation

$$\langle S^2\rangle_0 = \gamma M \tag{28}$$

for ideal coils is used. Using assumption 3 and eqs 27 and 28 yields

$$L_T' = \frac{6m}{b}\frac{d[Kc/I(q)]}{dq^2} \tag{29}$$

where, again, $m = 71$ is taken as the mass of a monomer, $b = 2.56$ Å is the contour distance between monomers, and $M = (Lm)/b$ has been used. Significantly, L_T' as determined by this method is independent of both polydispersity and all mass averages of the population. Furthermore, if m and b are known, the only significant sources of error, within the assumptions outlined, are the dn/dc value and the Kc/I data themselves, the former error being generally the largest.

Finally, a note concerning the rationale for this single concentration technique is warranted. First of all, the standard dilution technique ultimately gives $\langle S^2\rangle$ in terms of the slope of Kc/I vs q^2 divided by its $q = 0$ intercept. For the large $\langle S^2\rangle$ involved in this work the intercepts are very close to the origin and hence subject to large experimental uncertainties. The single concentration technique requires only the slope, which has much smaller error bars. Second, at low ionic strength isoionic dilutions of a polyelectrolyte are not practical, since the contribution of the polyelectrolyte counterions will continuously change the net solution ionic strength as it is diluted with a stock solvent of fixed C_s. Finally, the scattered intensity of polyelectrolyte solutions at low C_s is so weak that data obtained on successive dilutions become highly scattered after subtracting a solvent scattering level of nearly the same intensity as the total scattering.

Viscosity Measurements. Viscosity measurements were made in Strasbourg on a Contraves low-shear 30 Couette type viscometer interfaced to a Commodore computer. Temperature control was to within 0.01 °C of the 25 °C operating temperature. Intrinsic viscosities were determined by measuring the viscosity at given salt and polymer concentrations for a wide range of shear rates and then extrapolating to zero shear rate. These zero shear rate viscosities were then extrapolated to zero polymer concentration.

The concentration range was chosen to obtain a solution viscosity ranging between $1.5\eta_0$ and $2.5\eta_0$, where η_0 is the solvent viscosity. The lower limit is given by the accuracy of the measurements at zero shear rate, and the upper limit corresponds to the onset of chain overlap. Indeed the viscosity of the polymer solutions is given by the first three terms of the relation

$$\eta = \eta_0 + [\eta]c\eta_0 + k'[\eta]^2c^2\eta_0 \tag{30}$$

only if $c < c^* = 1/[\eta]$. η must always be less than 2.5, if the Huggins constant k' is around 0.5, no matter what the polymer and the experimental conditions are. We have only interpreted measurements when k' is of the order of 0.5, when the electrostatic screening was high enough to reduce the classical increase of viscosity at low polymer concentration.

Results and Discussion

Problem of Polyelectrolyte Aggregates at Low Ionic Strength. The presence of polymer aggregates in salt-free polyelectrolyte solutions deserves special mention, as neglect of their effects can radically change the data and interpretation of light scattering measurements.

Preliminary work with the AD series polymers indicated that salt-free solutions made from the dissolved granular powder showed residual traces of aggregates even after 8 h of centrifugation at 40 000g. The amount of aggregate was seriously effected by subjecting the salt-free solutions to different processes. If, for example, a salt-free solution was frozen, lyophilized, and reconstituted in pure water, the aggregate population was also very large. Ultrafiltration to remove any possible excess salt in the stock solutions was carried out in a pressurized cell with a 5000-MW cutoff filter on the outlet side, each exiting drop of solvent being replaced by a drop of pure deionized, triply distilled water. The resulting polymer solution after filtration was likewise full of aggregates and useless for light scattering measurements.

For the purposes of persistence length estimation, especially under low salt conditions where the low osmotic compressibility of the well-dispersed polyelectrolyte chains leads to very low scattering levels, the presence of aggregates can critically distort the light scattering data. It was thus found necessary to reduce the number of handling steps of the polymer in salt-free solution and to minimize the effects of any traces of aggregate left, primarily by filtration.

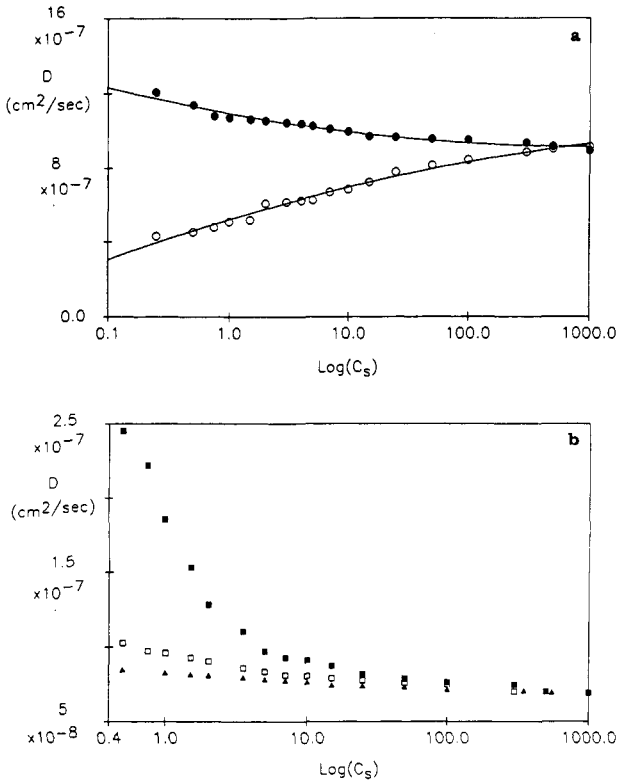

Figure 2. (a) Large and small D ($\theta = 90°$) vs log (C_s) from short and long autocorrelation decay components, respectively, when the autocorrelator was divided into halves (6- and 24-μs sample times) and each component was separately fitted. The solution was AD17 at 0.1 mg/mL, filtered through a 0.45-μm membrane instead of a 0.22-μm membrane: (●) short component; (○) long component. (b) D vs log (C_s) at $\theta = 90°$: (■) AD37 at 0.2 mg/mL; (□) 0.1 mg/mL; (▲) 0.1 mg/mL for AD17. All solutions were filtered through a 0.22-μm membrane. No small D component (long correlation) could be measured.

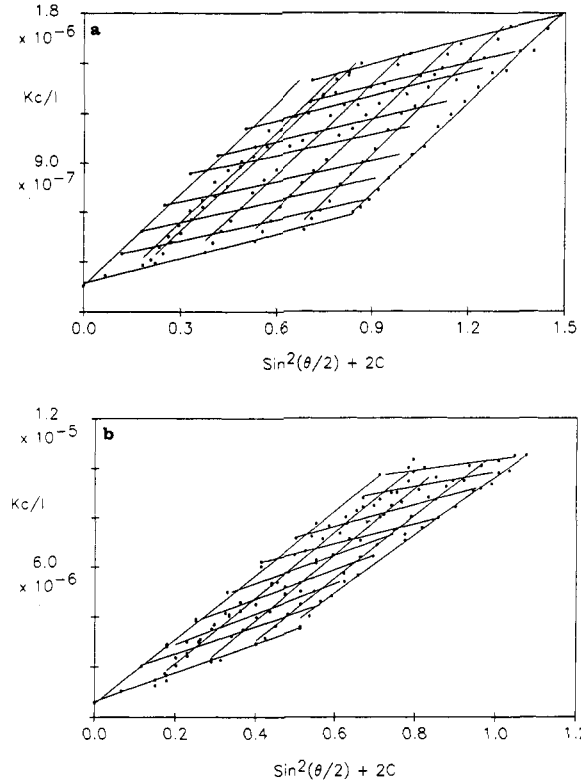

Figure 3. (a) "Zimm-type" plot for AD17 at 100 mM C_s. [AD17] = 0.5–0.075 mg/mL. (b) Zimm-type plot for AD37 at 10 mM C_s. [AD37] = 0.4–0.075 mg/mL.

If solutions were only centrifuged and not filtered, or filtered through membranes larger than 0.22 μm (e.g., 0.45 μm), there was evidence of a long relaxation time together with the short one. By dividing the correlator channels into halves, the first at 6 μs/channel and the second at 24 μs/channel, it was possible to roughly separate each component and get an estimate of the corresponding D. Figure 2a shows the long and slow components of D vs log (C_s) for an AD17 solution which was filtered through a 0.45-μm nylon membrane instead of through a 0.22-μm membrane. Although the long D component persists to high C_s and does not suddenly disappear, such a plot is reminiscent of those obtained for other polyelectrolytes, for which the low D is deemed to correspond to an extraordinary phase. Figure 2b shows D vs log (C_s) at different C_p after filtering through 0.22-μm filters. No low-D phase was found, nor did one reappear over a scale of days, so it was concluded that filtering through the proper pore-size membrane removed the long D phase.

With the exception of Figure 2a all data shown are for 0.22-μm-filtered solutions, which gave no trace of aggregates, or of an extraordinary phase, even at $\theta = 20°$. The lack of downward curvature of Kc/I at low angles, seen in Figure 1, for example, reveals how free of aggregates such solutions were.

Static Light Scattering. A "Zimm-type" plot of centrifuged, 0.22-μm-filtered AD17 in 100 mM C_s is shown in Figure 3a (Zimm-type because it assumes eq 27 for large, polydisperse random coils, rather than the usual conformation-independent treatment which is applicable when $q^2\langle S^2\rangle$ is less than about 3). With $\langle S^2\rangle^{1/2}$ around 1340 Å, $q^2\langle S^2\rangle$ is >3 above about $\theta = 44°$. Equation 27 for random coils is used to determine a number-average molecular weight M_n of about 3 million. Assuming $M_w/M_n \sim 2$, this is in reasonable agreement with measurements of $M_w = 5 \times 10^6$ using a 632-nm He–Ne laser at low angles for the polymers at high C_s.[54] A_2 is around 4.19×10^{-4}, and the perturbed γ is 0.31 ((Å² mol)/g).

Figure 3b shows a Zimm-type plot for centrifuged, filtered AD37 at 10 mM C_s. M_n for this plot is around 1.7 million, the perturbed γ is 2.16, and $\langle S^2\rangle^{1/2}$ is 2690 Å. A_2 is around 6.56×10^{-3} at this ionic strength. The approximate parellelity of the isoangular lines in Figure 3a,b indicates the validity of the assumption that $Q(q)$ is constant. Because the intercept is so close to the origin, it is not an accurate determination of the mass in this case, nor is it meant to be, since L_T' be eq 29 is independent of M_n or any other mass average. The M_n used subsequently in eq 27 to determine A_2 values is the 3×10^6 value determined under high C_s conditions and is assumed constant under all other C_s conditions.

Apparent persistence lengths were calculated according to eq 29 for all the AD series over a range of approximately 1 mM to 1 M C_s. An algorithm was used to find the exponent ν which gives the highest linear correlation coefficient in the relation $L_T' = a + bC_s^{\nu}$. The average best value for ν was -0.525 ± 0.06. We take $\nu = 0.5$ for convenience, and Figure 4 shows L_T' vs $C_s^{-0.5}$ for AD10, -17, -27, and -37. The y-intercepts yield the apparent intrinsic persistence lengths L_0' (infinite ionic strength limit of L_T'). "Apparent intrinsic persistence length" applies to this limit of L_T', since hard-core excluded-volume effects are still present at high salt as manifested by a large $A_{2,hs}$. It was fairly constant for the whole AD series and gave an average value of 27 ± 9 Å. This is in reasonable agreement with other reported values for fully ionized poly(acrylic acid)[13] and unhydrolyzed polyacrylamide.[27]

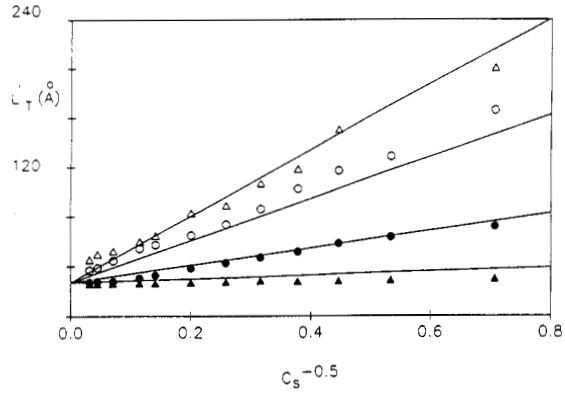

Figure 4. L_T' vs $C_s^{-0.5}$: (▲) AD10; (●) AD17; (○) AD27; (△) AD37. Lines are from eq 31.

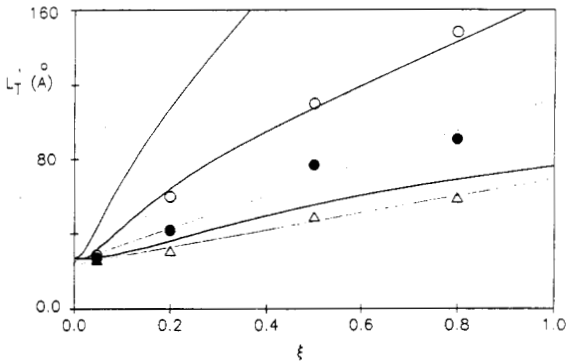

Figure 5. L_T' vs ξ from Figure 4 for different C_s: (○) 4 mM; (●) 16 mM; (△) 100 mM. The dark curves are from the excluded-volume calculations outlined in the text.

Since the average charge spacings run from about 150 Å for AD10 to about 10 Å for AD37, it is quite remarkable that the power law is so nearly constant for the whole series. It is not obvious that this should be so, especially as the charge spacing becomes more discrete toward low ionizations and hence becomes increasingly difficult to consider in terms of a smeared out, uniform charge density. Furthermore, the variations in average charge spacing for the different AD polymers crosses other scaling lengths, such as the Debye–Hückel screening length and the total persistence length, at different regimes of ionic strength. A recent Monte Carlo paper[16] has shown that, for polyelectrolyte chains with the same net charge, the L_T' is nearly the same for chains with randomly distributed charges and for uniformly distributed (smaller) charges. This finding lent support to the idea that treating a discretely charged polymer in terms of a smeared out uniform charge density may be actually quite a good approximation.

When points from the fitted lines from Figure 4 at different C_s were used, the same algorithm was used to calculate the best exponent ν for the relation L_T' vs ξ^ν. The average best value was 0.988 ± 0.05. For the simulations in ref 16, L_T' was also found to be linear in ξ. For convenience we take $\nu = 1.0$ and show the results in Figure 5. This leads to the following approximate expressions for apparent persistence length and $\langle S^2 \rangle$ for poly(acrylic acid) of charge density ξ and molecular mass M, in added salt C_s (mM)

$$L_T' \text{ (Å)} \approx 27 + 350\xi/C_s^{0.5} \tag{31}$$

and

$$\langle S^2 \rangle^{1/2} \approx [(Mb/3m)(27 + 350\xi/C_s^{0.5})]^{1/2} \tag{32}$$

Equation 31 is used to calculate the fitted lines for L_T' vs $1/C_s^{0.5}$ shown in Figure 4. It must be noted that the mass scaling implied in eq 32 results solely from the use of Mb/m to obtain L and was not tested in this work. Nevertheless, eq 32 gives good agreement with $\langle S^2 \rangle$ values measured by classical Zimm plot procedures for different mass fractions of hydrolyzed polyacrylamide.[30]

The first set of results shows that the experimental apparent persistence length does not follow the power laws in eq 3: it scales as $\xi C_s^{-0.5}$ while a scaling law of $\xi^2 C_s^{-1}$ is predicted in the absence of excluded-volume effects. Equation 3 works from within the Debye–Hückel approximation, assumes that the discrete charges along the polyelectrolyte chain can be approximated as a line charge of uniform density, and treats the polymer as an infinitely thin, flexible rod. Importantly, it also ignores long-range electrostatic forces. Since the AD molecules contain many statistical segment lengths under all conditions studied (e.g., for a mass of 5×10^6, N_k ranges from a high of about 3340 segments at high C_s to 240 at 1 mM for $\xi = 1.0$), it is probable that such long-range effects are significant.

First, we seek evidence for excluded-volume effects in the Kc/I light scattering data, which may in turn effect the interpretation of L_T' as a function of C_s. When the model introduced by Benoit[55] and elaborated on by Loucheux et al.[56] for the scattering from a nonideal coil is used, ref 12 gives the true persistence length L_T as

$$L_T = \frac{1}{2}\left[\frac{6^\epsilon m 2\epsilon\Gamma(\epsilon)}{b}\frac{d(Kc/I)}{dq^{2\epsilon}}\right]^{1/(2\epsilon-1)} \tag{33}$$

where Γ is the gamma function and $\epsilon = 1/\mu$, μ being the exponent in the mean-square separation $\bar{L}^2$ between two Kuhn segments p segments apart.

$$\bar{L}^2 = L_k^2 p^\mu \tag{34}$$

Thus μ measures the degree of the expansion due to excluded volume. For ideal coils $\mu = 1$, whereas for high excluded volume the Flory exponent of $\mu = 1.2$ may be approached. The Benoit model makes the questionable approximation that the distribution of L is still Gaussian. Taking the limiting form for $P(q)$ for large ν ($\equiv q^2 L_k^2 N_k^\mu/6$) given in ref 56 and substituting this $P(q)$ into eq 24 yields[12]

$$\frac{Kc}{I(q)} \cong \frac{\Gamma(2\epsilon)}{M_n[2\epsilon\Gamma^2(2\epsilon)]} + \frac{1}{2m_k\epsilon\Gamma(\epsilon)}q^{2\epsilon}(L_k^2/6)^\epsilon + 2A_2c \tag{35}$$

where $m_k = M/N_k$ is the mass of a Kuhn segment length. If the exponent ϵ can be found experimentally from the curvature of $Kc/I(q)$ vs q^2, then the slope of $Kc/I(q)$ vs $q^{2\epsilon}$ yields the true persistence length L_T via eq 33. ϵ can in turn be expressed in terms of the expansion parameter α_s appearing in eq 5 by

$$\alpha_s = [L/2L_T]^{\mu-1} \tag{36}$$

The same algorithm used to optimize the exponents for L_T' vs C_s and vs ξ was used in the attempt to find the exponents ϵ, in $Kc/I(q)$ data, such as shown in Figure 1. Values of ϵ between 0.7 and 1.1 were typically found and followed no systematic trends with either C_s or ξ. Values of ϵ showed an extreme sensitivity to the angular range of fitted points, to small amounts of noise in the data, and even to the inclusion of a single aberrant point. The L_T's in turn are extremely sensitive to small changes in ϵ, so that extremely high precision in determining ϵ is required for this technique to work. Visually at any rate, the Kc/I vs q^2 plots of Figure 1 are virtually straight lines, so that the light scattering data do not yield any clear indication of the excluded-volume effect.

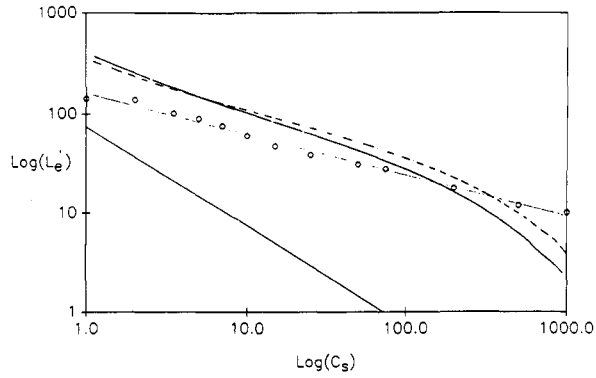

Figure 6. log (L_e') vs log (C_s) for AD27 (from Figure 4). The dashed line represents calculations according to excluded-volume correction with only electrostatic interactions ($A_{2,hs} = 0$), and the solid line represents calculations with both electrostatic and hard-core interactions ($A_{2,hs}$ = 0.000 28). The lower solid line is the unperturbed L_e given by relation 3: (○) from light scattering data.

A second procedure consists of calculating theoretical values of $\alpha_s = \alpha_s(\xi,C_s)$ and comparing the resulting theoretical values of L_T' ($=\alpha_s^2 L_T$, by eq 26) with the experimental values of L_T'.

The procedure for calculating $\alpha_s(\xi,C_s)$ is as follows: Extrapolations of the experimental values of A_2 and L_T' to infinite ionic strength are made from data such as those shown, for example, in Figures 4 and 6. We denote these high salt extrapolations as $A_{2,hs}$ and L_0', respectively. For the AD series L_0' = 27 Å and represents the apparent intrinsic persistence length and is equal to L_0 only if $A_{2,hs} = 0$. Since for the AD series $A_{2,hs} \sim 2.8 \times 10^{-4}$, $L_0' \neq L_0$. Knowledge of L_0' and $A_{2,hs}$, however, allows $\alpha_{s,hs}$, and hence L_0 ($=L_0'/\alpha_{s,hs}^2$), to be found, if the theories summarized in eqs 6–11 are used. Namely, a search for the high $C_s\beta_0$ value can be made, finding $\alpha_{s,hs}$ at each β_0 value according to

$$1/\alpha_{s,hs}^2 - 1/\alpha_{s,hs}^4 = \frac{134}{105}\left(\frac{L}{2L_0'}\right)^{1/2}\left(\frac{3}{8\pi L_0'^2}\right)^{3/2}\left[1 - 0.885\left(\frac{\alpha_{s,hs}^2 L}{2L_0}\right)^{-0.462}\right]\beta_0 \quad (37)$$

and then calculating A_2 from eqs 6 and 8 by

$$A_2 = \left[\frac{N_A \alpha_{s,hs}^4 L^2}{8M^2 L_0'^2}\right]\beta_0 h_0(\tilde{z}_{hs}) \quad (38)$$

The value of β_0 is searched in this way until $A_2 = A_{2,hs}$ in eq 38.

Here

$$\tilde{z}_{hs} = \left[\frac{3}{8\pi L_0'^2}\right]^{3/2}\left[\frac{L}{2L_0'}\right]^{1/2}\alpha_{s,hs}^4\beta_0 \quad (39)$$

For the AD series $\alpha_{s,hs}^2 = 1.407$, L_0 = 13.6 Å, and β_0 = 1653 Å^3. As a rough check on β_0 it is interesting to note that the excluded volume for a cylinder of length L = 13.6 Å and d = 5 Å is 1452 Å^3 ($=\pi d L^2/2$).

With $\alpha_{s,hs}$ found, $\alpha_s(\xi,C_s)$ is then calculated at each (ξ,C_s) by using $L_T = L_0 + L_e$ ($=L_k/2$) to compute β_{el} in eq 7. L_e is computed by eq 3. The rod diameter was taken as 5 Å in eq 7. z in eq 6 is then calculated with $\beta = \beta_{el} + \beta_0$. Finally, $\alpha_s^2(\xi,C_s)$ is found with this value of z via eq 8; hence, the theoretical values of $L_T'(\xi,C_s)$ and $A_2(\xi,C_s)$ (via eqs 9–11) are found. Theoretical L_e' values are obtained by subtracting off L_0' (27 Å) from the theoretical L_T'.

The results of these calculations are shown in Figures 5–7. Figure 5 gives the theoretical L_T' values vs ξ for C_s = 4, 16, and 100 mM. The agreement with the data points is good only for C_s = 100 mM.

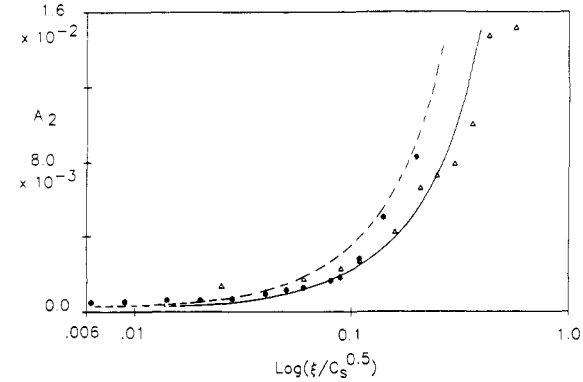

Figure 7. A_2 vs log ($\xi/C_s^{0.5}$): (●) AD17; (△) AD37. The curves represent calculations with both electrostatic and hard-core excluded-volume interactions ($A_{2,hs}$ = 0.000 28), as described in the text; the dashed line is for AD17; the solid line is for AD37.

The unconnected points in the log (L_e') vs log (C_s) plots in Figure 6 represent the experimental apparent electrostatic persistence lengths L_e', obtained by subtracting L_0' (27 Å) from the experimental L_T'. The upper solid line in Figure 6 shows the theoretical L_e' calculated by the above procedure. The agreement with the data is qualitatively good, especially when compared with L_e from eq 3, which is shown on the same graph (lower solid line) and appears qualitatively unrelated to the experimental L_e'. As a further comparison, the dashed line in Figure 6 represents the theoretical L_e' if it is assumed that $A_{2,hs}$ = 0, as was implictly done, for example, for bacterial hyaluronate in ref 12 (even though $A_{2,hs} \sim 0.0015$ for hyaluronate). The differences in the two upper curves (solid and dashed) are not striking, so that inclusion of β_0 is not a major consequence in terms of calculating L_e'. Similar L_e' vs C_s behavior was obtained for the other AD molecules.

Figure 7 shows A_2 vs log ($\xi/C_s^{1/2}$) for AD17 and AD37, computed from the Kc/I data according to eq 7, along with the theoretical values calculated by the above procedure. The agreement is quite good, and better than simply adding $A_{2,hs}$ to the electrostatic portion of A_2.[57]

Taken together, the good predictions of A_2 and the sometimes qualitatively good predictions of L_e' lend support to the notion that excluded-volume effects, especially of the electrostatic sort, strongly affect the dimensions and interactions of the AD polyelectrolytes and may be at least partially at root in the difference between the unperturbed L_e from eq 3 and the experimental L_e'. We do not attempt to evaluate here the approximations involved in eqs 6–11 nor the predictions of alternative theories but admit that other theories and/or combinations might yield yet better agreement of L_e' with the data.

Dynamic Light Scattering Results. The behavior of D vs C_s for 0.45- and 0.22-μm-filtered AD solutions was shown in parts a and b of Figure 2, respectively.

Figure 8 shows D vs [AD17] at θ = 90° at C_s values of 5, 10, and 1000 mM and vs [AD37] at θ = 90° at C_s = 10 and 1000 mM. Again, all solutions were 0.22-μm-filtered to eliminate any extraordinary phase and/or aggregates that might distort the low-angle data. Interestingly, they all extrapolate to the same y-intercept, which is denoted as D_0, the diffusion coefficient of the polyelectrolyte at zero polyelectrolyte concentration. Since the dimensions of these molecules are on the order of the range of the reciprocal wave number q^{-1}, internal flexional modes may show up in the scattered intensity autocorrelation function.

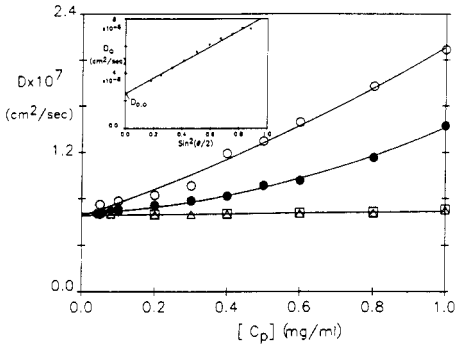

Figure 8. D vs [AD17] at $\theta = 90°$ for different C_s: (○) 5 mM; (●) 10 mM; (□) 1000 mM. Also shown is D vs [AD37] for C_s: (♦) 10 mM; (△) 1000 mM. The inset to Figure 8 shows averaged D_0 (D extrapolated to $C_p = 0$) vs $\sin^2(\theta/2)$ for the different ADs at different C_s (they all converged within error bars), showing that both D_0 and $D_{0,0}$ are independent of C_s and ξ.

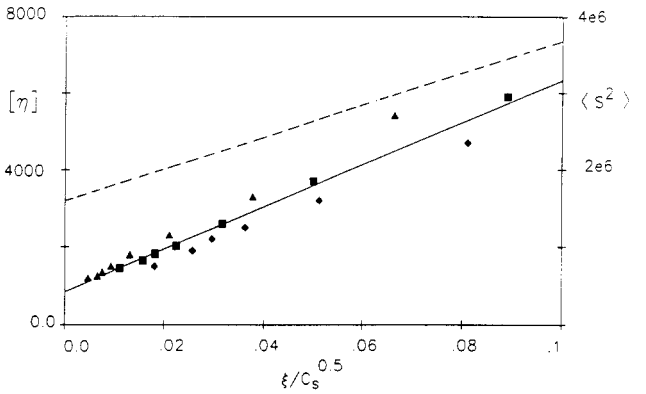

Figure 9. $[\eta]$ vs $\xi/C_s^{0.5}$: (♦) AD17; (■) AD27; (▲) AD37. The dashed line corresponds to the right-hand axis and represents $\langle S^2 \rangle$ obtained from the static light scattering experimental eq 32 for $M = 5 \times 10^6$.

Extrapolating D_0 to $\theta = 0°$ should eliminate any contribution from internal modes, should they exist.

The inset to figure 8 shows D extrapolated to $C_p = 0$ at each angle for the whole AD series, over $C_s = 1$ mM to 1 M, plotted vs $\sin^2(\theta/2)$. All AD samples yielded the same value at each angle, within error bars. Extrapolating these values to $\theta = 0°$ yielded a $C_p = 0$ and $\theta = 0°$ diffusion coefficient, $D_{0,0}$, of 2.5×10^{-8} cm^2/s, which gives a corresponding R_H of 1000 Å when calculated by the Stokes–Einstein equation for spheres. The positive slope of D vs q^2 may just as well result from polydispersity rather than internal modes. No matter what phenomena cause the slope, the fact remains that D_0 is independent of C_s and ξ for all θ. The fact that $D_{0,0}$ is independent of C_s and ξ suggests that the AD polyelectrolyte coils may be at least partially draining. It can be roughly seen from the data of Skazka and Tarasova,[18] who have found the same independence of $D_{0,0}$ from C_s, however, that D_0 scales roughly as $M^{0.5}$ and not as M, as would be expected for total free draining. Thus it seems difficult to assign this constancy of $D_{0,0}$ to a total free-draining condition.

For nondraining coils $R_H = 0.665\langle S^2 \rangle^{1/2}$. $D_{0,0}$ represents a z-average of the polymer distribution. Since M_z is not known, we use $M_w = 5 \times 10^6$ as a lower limit. Then, for this mass, $\langle S^2 \rangle^{1/2}$ should range, according to eq 32 from at least 1270 to 3880 Å, in going from 100 mM for any ξ to 1 mM for $\xi = 0.77$ (AD37). This gives an upper limit of the ratio of $R_H/\langle S^2 \rangle^{1/2}$ over this $\xi/C_s^{0.5}$ range of 0.79–0.26. For $C_s = 1000$ mM the upper limit of 0.79 for $R_H/\langle S^2 \rangle^{1/2}$ is not too different from the expected nondraining value of 0.665, and the agreement would be improved if M_z were known. In the case of unhydrolyzed polyacrylamide, the expected nondraining behavior was found over a large range of molecular weights.[29,54,58] Although an argument might be made for AD not being in the random-coil limit, it is important to point out that N_k ranges from 240 to over 3000 as ξ and C_s are varied. Furthermore, Douglas and Freed,[41] on the basis of renormalization group theory, state that nondraining requires the proportionality of α_s and α_H.

The dominant role of the electrostatic effects on the polyelectrolyte expansion may also be responsible for the striking discrepancy between the experimental constancy of $D_{0,0}$ and the nondraining prediction of direct inverse proportionality between $D_{0,0}$ and $\langle S^2 \rangle^{1/2}$. Being a "soft" interaction, the electrostatic potential responsible for the electrostatic excluded volume may be expected to interact much less strongly with the flow of solvent than "hard" steric monomer volumes. Electrostatic effects may be responsible for the discrepancy between experiments and theoretical predictions.

Reference 12 showed behavior similar to that in Figure 8 for hyaluronate of mass around 1 million, likewise suggesting a partial free-draining condition. Since L_0' was around 87 Å, indicating a fair degree of intrinsic stiffness, it was suggested that the "open"-coil structure of hyaluronate made such partial draining plausible. For the AD series polymers, however, L_0' is only around 27 Å, indicating a much more flexible structure, and yet partial free draining seemingly still applies. That the independence of R_H from $\langle S^2 \rangle^{1/2}$ is not merely an artifact of the methods used in this work is supported by a recent finding[57] using the same methods for proteoglycan monomers (dense, branched structures involving short glycosaminoglycan chains covalently linked to a protein backbone). In that case $R_H \approx 0.7\langle S^2 \rangle^{1/2}$ over to 1000 mM C_s, and hence nondraining conditions apply for the proteoglycans. Furthermore, for poly(styrene sulfonate),[59] there appeared to be three regimes; at high C_s $1/D_{0,0} \propto \langle S^2 \rangle^{1/2}$, at intermediate C_s (30–150 mM) $1/D_{0,0}$ dropped below $\langle S^2 \rangle$, and below about 30 mM C_s $1/D_{0,0}$ was independent of C_s. $D_{0,0}$ in any regime, however, followed $M^{0.5}$, thus virtually ruling out any simple total free-draining explanation for the low C_s regime.

Viscosity Results. Figure 9 shows plots of the measured intrinsic viscosity versus the parameter $\xi/C_s^{0.5}$. Also shown is $\langle S^2 \rangle$ with dimensions shown on the right-hand axis. $[\eta]$ is a fairly linear function of this parameter, but the curves corresponding to the different AD do not superimpose well. $[\eta]$ at all $\xi/C_s^{0.5}$ is slightly lower for AD37 than for the two other samples. It has been well-known experimentally for a long time that $[\eta]$ of linear polyelectrolytes varies as $C_s^{-0.5}$. The dependence on ξ is less clear. From the theories of Fixman et al.[36] and Odijk and Houwaart[35] and by using the Yamakawa–Kurata eq 17 and the Yamakawa–Tanaka[17] expression for the dependence of α_s on z, Medjahdi[53] has shown that the variation of $[\eta]$ as a function ξ has a slight downward curvature. This variation can be considered, however, as linear to a first approximation, as long as $\xi < \xi_c$, the critical Manning charge parameter corresponding to the onset of the ionic condensation.[34] The more pronounced curvature often found for hydrolyzed polyacrylamide or copolymers[30-32,53] has been interpreted by Zema and Kowblansky[32] as due to condensation occurring for ξ values lower than ξ_c. We will neglect this possible phenomenon in this paper.

In Figure 10, the apparent persistence lengths calculated from the Yamakawa and Fujii[42] eq 14 can be compared with those found from light scattering experiments by eq 29. There is fairly good agreement between the two sets

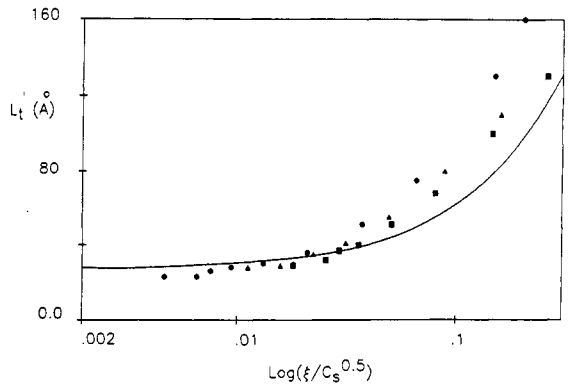

Figure 10. L_T' vs log ($\xi/C_s^{0.5}$) from viscosity data via eq 16: (■) AD17; (▲) AD27; (●) AD37. The solid line is from the L_T' eq 31 obtained by static light scattering.

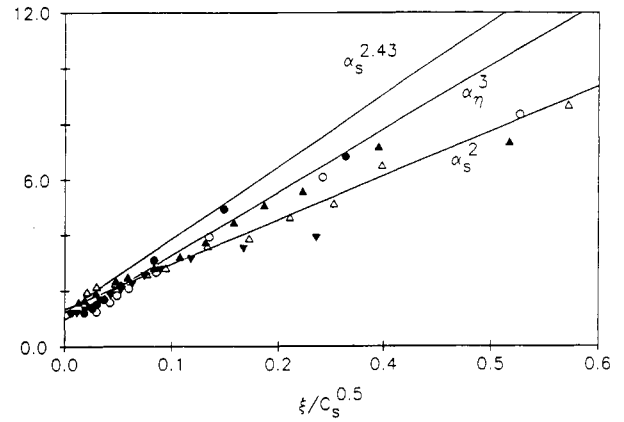

Figure 11. $\alpha_s^{2.43}$ vs $\xi/C_s^{0.5}$ in top line. Experimental points for α_η^3 vs $\xi/C_s^{0.5}$: (●) AD27; (○) AD17 (middle line is fit to these data). α_s^2 vs $\xi/C_s^{0.5}$ from the experimental data: (▼) AD17; (△) AD27; (▲) AD37 (lower line is the fit to these data).

of data for the low values of $\xi/C_s^{1/2}$. Interestingly, this formula assumes strong hydrodynamic interactions[42] and hence also excludes the possibility of total free draining. The divergence between the L_T' values determined by viscosity and light scattering at higher values of $\xi/C_s^{0.5}$ may reflect increasing deviations from the strong type of hydrodynamic interactions assumed by the Yamakawa–Fujii theory in deriving eq 14.

It is interesting to compare the viscosimetric expansion factor defined by eq 16 with the static one. We observe that $\langle S^2\rangle$ (and α_s^2) and $[\eta]$ (and α_η^3) are both proportional to $\xi/C_s^{0.5}$. Then from the Weill–des Cloizeaux theory[48] (eqs 19 and 20), one may expect that R_H and α_H are independent of ξ and c_s, as observed experimentally. There may be self-consistency between the three sets of experiments. However, if this is true, $\alpha_\eta^3 = [\eta]/[\eta]_0$ must be equal to α_s^2 and not just proportional. Figure 11 shows that α_η^3 is generally higher than α_s^2 but does not exceed the values expected from the Yamakawa–Kurata relation, eq 18. If one assumes that the discrepancies between the values of α_η and α_s are due partially to experimental errors and partially to polydispersity, these results may lend some support, at least for small values of $\xi/C_s^{0.5}$, to the universality of the Weill–des Cloizeaux eq 20, which should be applicable even when the friction coefficient or the hydrodynamic radius of gyration do not follow the classical nondraining behavior.

Conclusions

$\langle S^2\rangle$ and L_T' of variably ionized polyacrylate vary as $\xi/C_s^{0.5}$. $[\eta]$ also scales as $1/C_s^{0.5}$ but is less clearly proportional to ξ. The L_T' values extracted from $[\eta]_0$ via the Yamakawa model are in good agreement with those obtained independently by static light scattering.

In contrast, $D_{0,0}$ (and R_H) appears independent of $\xi/C_s^{0.5}$ and approaches the expected nondraining result ($R_H = 0.665\langle S^2\rangle^{1/2}/12$) only at very low $\xi/C_s^{0.5}$, i.e., at high salt and or low charge density, where the polyelectrolyte behaves more like a neutral polymer. A partial draining condition may be involved in the constancy of R_H, although total free draining in the simplest sense seems improbable due to the lack of evidence for a scaling of $f \propto M$.

The dependence of L_T' on $\xi/C_s^{0.5}$ deviates from unperturbed persistence length theory, which predicts that L_e varies as C_s^{-1} and as ξ. Since long-range electrostatic effects are certainly important, corrections based on electrostatic excluded-volume theories are made and found to improve significantly the agreement with experiment. Similarly, the same electrostatic excluded-volume theories give a good account of the A_2 behavior. There is, however, no direct experimental evidence in the static light scattering data for the electrostatic excluded-volume effect, so that its existence still remains inferred by the improved agreement it gives between the experiments and the unperturbed theories. Direct measurements of L_T, perhaps by neutron scattering, would help to separate the short- and long-range effects on polymer dimensions.

What seem to be fairly stable, entangled polymer aggregates exist at low ionic strength and give a low-D diffusional phase, reminiscent of the extraordinary phase reported for many polyelectrolytes. These aggregates, and hence the low D and any appearance of an extraordinary phase, can be removed by filtration through sufficiently small pore size membranes. This topic is treated more fully in a recent work,[60] in which abrupt losses of long D components vs. C_s were found for certain polyelectrolytes.

Acknowledgment. Support for this work came from NATO Collaborative Research Programme CRG-900620, from the United States National Science Foundation Grant DMB 8803760, and from the French Centre National de Recherche Scientifique. We thank Gilbert Weill and Michel Rawiso for many helpful discussions.

References and Notes

(1) Hermans, I. J. *Recl. Trav. Chim. Pays-Bas* **1949**, *68*, 859.
(2) Flory, P. J. *J. Chem. Phys.* **1953**, *21*, 162.
(3) Katchalsky, A.; Lifson, S. *J. Polym. Sci.* **1953**, *11*, 409.
(4) Fixman, M. *J. Chem. Phys.* **1964**, *41*, 3772.
(5) Nagasawa, M. *J. Polym. Sci., Polym. Symp.* **1975**, *19*, 1.
(6) Noda, I.; Tsuge, I.; Nagasawa, M. *J. Phys. Chem.* **1970**, *74*, 710.
(7) Odijk, T. *J. Polym. Sci., Polym. Phys. Ed.* **1977**, *15*, 477.
(8) Skolnick, J.; Fixman, M. *Macromolecules* **1977**, *10*, 944.
(9) Muraga, Y.; Noda, I.; Nagasawa, M. *Macromolecules* **1985**, *18*, 1576.
(10) Plestil, J.; Ostanevich, Y. M.; Bezzabotonov, V. Y.; Hlavata, D.; Labsky, J. *Polymer* **1986**, *27*, 339.
(11) Fisher, L. W.; Sochor, A. R.; Tan, J. S. *Macromolecules* **1977**, *10*, 5, 9558.
(12) Ghosh, S.; Xiao, L.; Reed, C. E.; Reed, W. F. *Biopolymers* **1990**, *30*, 1101.
(13) Tricot, M. *Macromolecules* **1984**, *17*, 1698.
(14) Trimm, H. H.; Jennings, B. R. *Biochem. J.* **1983**, *213*, 671.
(15) Reed, C. E.; Reed, W. F. *J. Chem. Phys.* **1990**, *92*, 6916.
(16) Reed, C. E.; Reed, W. F. *J. Chem. Phys.* **1991**, *94*, 8479.
(17) Yamakawa, H. *Modern Theory of Polymer Solutions*; Harper and Row: New York, 1971.
(18) Skazka, V. C.; Tarasova, G. V. *Vysokomol. Soedin., Ser. B* **1978**, *20*, 97.
(19) Lin, S. C.; Lee, W. I.; Schurr, J. M. *Biopolymers* **1978**, *17*, 1041.
(20) Nikolai, T.; Mandel, M. *Macromolecules* **1989**, *22*, 2348.
(21) Fulmer, A. W.; Benbasat, J. A.; Bloomfield, V. A. *Biopolymers* **1981**, *20*, 1147.
(22) Drifford, M.; Dalbiez, J. P. *J. Phys. Lett.* **1985**, *46*, L-311.
(23) Förster, S.; Schmidt, M.; Antonietti, M. *Polymer* **1990**, *31*, 781.
(24) Drifford, M.; Dalbiez, J. P. *Biopolymers* **1985**, *24*, 1501.

(25) Truong, D. N.; Galin, J. C.; François, J.; Pham, Q. T. *Polymer* **1986**, *26*, 467.
(26) Kulicke, W. M.; Kneinshe, R.; Klein, J. *Prog. Polym. Sci.* **1982**, *8*, 373.
(27) François, J.; Sarazin, D.; Schwartz, T.; Weill, G. *Polymer* **1979**, *20*, 969.
(28) Schwartz, T.; Sabbadin, J.; François, J. *Polymer* **1981**, *22*, 609.
(29) François, J.; Schwartz, T.; Weill, G. *Macromolecules* **1981**, *13*, 609.
(30) Schwartz, T.; François, J. *Makromol. Chem.* **1981**, *182*, 2757.
(31) Kulkarni, R. A.; Gundiah, S. *Makromol. Chem.* **1984**, *185*, 957, 969, 983.
(32) Zema, P.; Kowblansky, M. *Macromolecules* **1981**, *14*, 1448, 1451.
(33) Benoit, H.; Doty, P. *J. Phys. Chem.* **1953**, *57*, 958–963.
(34) Manning, G. S. *J. Chem. Phys.* **1969**, *51*, 924.
(35) Odijk, T.; Houwaart, A. C. *J. Polym. Sci., Polym. Phys. Ed.* **1978**, *16*, 627.
(36) Fixman, M.; Skolnick, J. *Macromolecules* **1978**, *11*, 863.
(37) Gupta, S. K.; Forsman, W. L. *Macromolecules* **1972**, *5*, 779.
(38) Kirkwood, J. G.; Riseman, J. *J. Chem. Phys.* **1948**, *16*, 565.
(39) Rouse, P. E. *J. Chem. Phys.* **1953**, *21*, 1272.
(40) Wang, S.; Douglas, J. F.; Freed, K. F. *J. Chem. Phys.* **1987**, *87*, 1346.
(41) Douglas, J. F.; Freed, K. F. *Macromolecules* **1984**, *17*, 2354.
(42) Yamakawa, H.; Fujii, M. *Macromolecules* **1974**, *7*, 128.
(43) Oseen, C. W. *Hydrodynamik Akademische Verlagsgesellschaft*; Leipzig, 1927.
(44) Burgers, M. *Second Report on Viscosity and Plasticity of the Amsterdam Academy of Sciences*; New York, 1938.
(45) Flory, P. J.; Fox, T. G., Jr. *J. Am. Chem. Soc.* **1951**, *73*, 1904.
(46) Kurata, M.; Yamakawa, H. *J. Chem. Phys.* **1958**, *29*, 311.
(47) Yamakawa, H.; Kurata, M. *J. Phys. Soc. Jpn.* **1958**, *13*, 94.
(48) Weill, G.; des Cloizeaux, J. *J. Phys. (Orsay, Fr.)* **1979**, *40*, 99.
(49) Odijk, T. *Biopolymers* **1979**, *18*, 3111.
(50) Sharp, P.; Bloomfield, V. A. *J. Chem. Phys.* **1968**, *48*, 2149.
(51) Boutin, J.; Contat, S. (to Rhone-Poulenc Ind.) French patent 249217, 1980.
(52) Reed, C. E.; Xiao, L.; Reed, W. F. *Biopolymers* **1989**, *28*, 1981.
(53) Medjahdi, G. Ph.D. Thesis, Universite Louis Pasteur, Strasbourg, France, 1989.
(54) Schwartz, T.; François, J.; Weill, G. *Polym. Commun.* **1980**, *21*, 247.
(55) Benoit, H. *C.R. Acad. Sci.* **1957**, *245*, 2244.
(56) Loucheux, C.; Weill, G.; Benoit, H. *J. Chim. Phys.* **1958**, *55*, 540.
(57) Xiao, L.; Reed, W. F. *J. Chem. Phys.* **1991**, *94*, 4568.
(58) Duval, M.; François, J.; Sarazin, D. *Polymer* **1985**, *26*, 399.
(59) Peitzsch, R. M.; Burt, M.; Reed, W. F. *Macromolecules*, in press.
(60) Ghosh, S.; Peitzsch, R. M.; Reed, W. F., manuscript submitted.